# Power Efficient Long Range Drone Networking System for UAV Detection

Gihwan Kim
*Computer science and Engineering*
*Chungnam National University*
Daejeon, Republic of Korea
201701981@o.cnu.ac.kr

Soonchan Kwon
*Software engineering*
*Chonnam National University*
Gwangju, Republic of Korea
182575@jnu.ac.kr

Nahyeong Kim
*Computer science and Engineering*
*Chungnam National University*
Daejeon, Republic of Korea
nhkim5697@o.cnu.ac.kr

Nawon Kim
*Computer Engineering*
*Chonnam National University*
Gwangju, Republic of Korea
201600@jnu.ac.kr

Karteikay Dhuper
*Computer and Information Technology*
*Purdue University*
West Lafayette, Indiana
kdhuper@purdue.edu

Prakshi Chander
*Cybersecurity*
*Purdue University*
West Lafayette, Indiana
pchander@purdue.edu

*Abstract*—In recent years, technological advancements in Unmanned Aerial Vehicles (UAV) have removed barriers to entry on drone usage for the public. While this has led to the growth of the drone industry it has also provided terrorists with easier access to drones. Rising threats of malicious drones have raised the importance of a Counter Drone System (CDS). Traditional CDSs use a variety of physical sensors and technologies to detect hostile drones and react efficiently, however, these methods have their own set of constraints, such as high power consumption and short operational range. This paper proposes a power-efficient long range CDS composed of a LoRa mesh network and on-device Machine Learning (ML). LoRa provides low-power and long range communication and the multi-hop feature of the mesh network expands the coverage of the network. Applying TinyML on the Micro-Controller unit is reasonable. The implemented system achieves a satisfactory communication range, a successful operation of the UAV detection and a power consumption which is similar to that of typical MCU.

*Index Terms*—Counter Drone Systems, Counter UAV system, Unmanned aerial vehicle (UAV), UAV detection, Data communication, Wireless communication

## I. INTRODUCTION

The reduction in manufacturing cost and physical design associated with drones has increased accessibility to numerous industries seeking to utilize unmanned aerial vehicles (UAVs) for their personal needs. The impact of these improvements has invigorated a variety of commercial UAV fields such as transportation, delivery services, and disaster monitoring [1]. As the UAV industry grows, the threats of hostile drones increase. Occurrences of adversarial drone incidents have been observed around the world as reported by the media. In Saudi Arabia, the Houthi rebels in Yemen actively exploited technologically improved drones to attack oil treatment facilities, oil supply facilities, and cities in 2019 and 2021 [2]. In 2022, Russian kamikaze drones struck Ukraine. Since mid-October 2022, Russia has initiated countless drone attacks on Ukraine [3]. Recently Israel executed a drone attack on an Iranian defense factory [4]. These violent incidents demonstrate the necessity

for a Counter Drone System (CDS) to mitigate the impacts of adversarial drones on the functioning of society.

Ground Counter Drone Systems (GCDS) that detect aerial enemies on the ground in a fixed location have the limitations of flexible response. Airspace Counter Drone Systems (ACDS), on the other hand, use drones to observe wide areas in the air regardless of geographic limitations. The strategy of ACDS triggers more power consumption causing limited operation time and distance. Conventional methods that supply additional power [5], [6] reduce these limitations. However, these methods inevitably have heavier payloads, which means that the operation time and the range of the Counter Drone System are also subject to restrictions.

The purpose of this paper is to design an enhanced long range Counter Drone System that leverages a power-efficient network structure while performing drone detection. In order to achieve this goal, each drone is equipped with a long range wireless platform and an on-device detection component. A Mesh network is utilized for wide area coverage and to ensure robustness to damage via multi-hop. Since multiple hops constitute the network, data is relayed among hops and damaged hops are replaced by regular ones. A drone takes the visual data from the camera to detect adversarial drones and to execute inference with the detection model directly from the device. Therefore, the prediction process eliminates redundant data transmission that sends large visual data to a central computing system. This process enables the drone industry to build an efficient network for CDS. [TODO brief conclusion]

## II. RELATED WORKS

The immobile nature of a GCDS alleviates size, weight, and power constraints and allows for a more resource-intensive system that uses more accurate and powerful devices, radars, and cameras. The radar recognizes unidentified objects that reflect electromagnetic radiation of radar [8]. Cameras are used
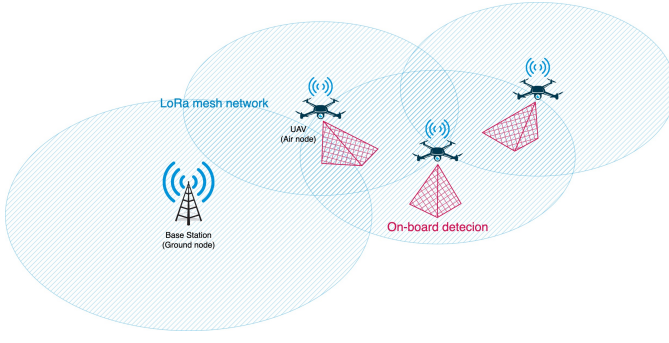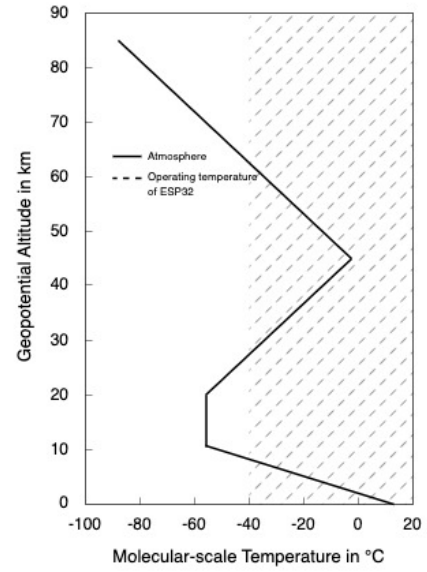
Fig. 1. System overview. Adapted from [25]



Fig. 2. Comparison graph between molecular-scale temperature as a function of geopotential altitude in [17, Fig. 3] and operating temperature of ESP32

to capture thermal and visual image of drones. The images used to identify characteristic of drones [9]. Despite all this, the fixed location of a ground system has limited visibility and response to the drones.

Airspace Counter Drone Systems consist of specific drones which loaded sub systems. The drones provide mobility for the system to universally detect and respond to other drones. An optical-based approach system [10] not just detects drones using visual data but also adds functions for tracking. Research from NASA [11] is a system focused on searching, detecting and tracking. In this system, a small UAV uses a Wi-Fi link to transmit the live video streams of flight telemetry data and its front camera to the ground computer. The ground system, which is off board computer, receives the data and runs all the processes such as core software components. The centralized computing structure leads to have high computing resource and data transmission latency for transmitting and processing large data on the off-board computer.

As it uses Wi-Fi links, it is also important to select the appropriate wireless communication protocol to improve the performance of certain drone systems. A swarm of UAVs [34] that builds a wireless infrastructure using high-speed Wi-Fi has been proposed. They form a mesh network and provide up to 160Mbps of wireless communication over a coverage of about 200m. It has adequate throughput for large-scale data transmission, whereas it results in the limit of maximum distance [35].

The existing CDSs have some difficulties with immobility, high computing source, limited distances. As the solution to relieve these constraints, a system designed to enable low power consumption and long range communication is proposed.

## III. METHODOLOGY

The system to relieve the problems of the original ACDS is shown in Fig. 1. It is designed by utilizing the following tools: ESP32, LoRa modulation, Mesh network, TinyML, object detection model.

### A. ESP32-WROVER

ESP32-WROVER is manufactured as powerful and generic MCU based on ESP32. ESP32 has ability to operate in a variety of environments stably [12], [13]. Kamikaze drones fly at an altitude of 1km above the ground until they reach their target [15] and bomb carrying drones operate at a few hundred meters above ground [16]. Fig. 2 shows atmosphere temperature below 5km where terror attack is conducted is -25–17°C. As ESP32 operate successfully under the -40–125°C environment, ESP32 is suitable for a MCU of CDS. ESP32 supplies several power modes. The active mode operates all modules with a peak performance. The modem-sleep mode disables unnecessary modules, such as unused Radio Frequency (RF) modems, and the deep-sleep mode reduces the power consumption to the maximum. Whereas the active mode consumes 240mA, the modem-sleep mode consumes 20–68mA and the deep-sleep mode consumes 10μA [12]. Due to battery life, the absence of power modes is beneficial.

### B. LoRa modulation

LoRa stands for a wireless modulation scheme derived from Chirp Spread Spectrum (CSS) [18]. LoRa modulation encodes data bits by chirps with linear variation of frequency. Major characteristic of chirp is constant envelop that enables efficient low-power modulation. The energy that is consumed to make a same link budget is saved compared to a traditional modulation, such as Frequency Shift Keying (FSK), due to the processing gain of LoRa [18]–[20].

The broadband chirp pulse is immune to multipath propagation that interferes with a wanted radio signal and fading that is attenuate variation of a radio signal. The high time-bandwidth product and its asynchronous nature provide robustness to Radio Frequency Interference (RFI) [21]. The out-of-band selectivity of receiver is shown as 90dB and co-channel rejection is shown as 20dB or more. On the other hand, FSK features 50dB and -6dB respectively. The figures of LoRa

are outstanding compared to FSK. This excellent immunity to multipath, fading and RSI in link budget lead 4 times or beyond enhancement in communication range [18], [22], [23].

LoRa commonly use sub-gigahertz (Sub-GHz) bands (e.g. 915MHz, 868MHz and 433MHz). Sub-GHz bands signals are not absorbed by physical matter as much as GHz bands (e.g. 2.4GHz, 5GHz) [24]. Moreover, they generate low receiver sensitivity (up to -140dBm) which allow receiver to detect weak signals as the sensitivity of receiver is inversely proportional to channel bandwidth. Thus LoRa is suitable for low-power and long range communication. Physical and electrical configurations of LoRa affect the performance of LoRa. The configurations consist of four parameters. The parameters are set depend on the purpose of usage as there are no parameters that produce only gainful results. All changes of parameters have a trade-off [26].

*1) Transmission power:* Transmission power stands for the strength of transmitted signals. The higher transmission power enables a higher link budget while power consumption for transmission increases.

*2) BandWidth (BW):* BW represents the frequency range of chirp which is modulated. Narrower BW result in longer range and slower transfer rate.

*3) Coding Rate (CR):* LoRa provides a error correction scheme to improve the robustness of signals from a interference. Payload includes actual data and error-correcting data which is used to verify the error. CR defines the ratio of actual data to error-correcting data. Increasing the CR makes the signal more reliable, however the data rate decreases.

*4) Spreading Factor (SF):* SF represents how many chirps is used per a symbol. The higher SF increase the sensitivity of receiver.

*C. Mesh network*

Mesh network consists of a series of communication nodes. They are interconnected over wireless links using multiple wireless technologies [27]. It makes all nodes be connected to all other nodes. Each node has routing functions and communicates with only the nearby nodes. Even if one node fails, other paths will be used to transmit the data because of its connectivity. In Fig. 3, node B sends the data to node E using the route, which is (B→A→D→E). If node D is blocked, node A will transmit the data using the new route, which is (B→C→F→E). So this network provides connection continuously through rerouting if there is a blocked route by hopping the data from node to node until it reaches its destination [28], [29].

In addition to its robustness, mesh network increase the network coverage. U.S. Department of Defense told that mission coverage is one of the considerations for the development of UAV systems [14]. Each node turns on the power and discovers other nodes within a certain range for large coverage. So it simplifies extending the coverage by adding a new node to existing coverage. According to the characteristics of multi-hop communication, network coverage will be expanded without difficulty in channel capacity, which overcomes the
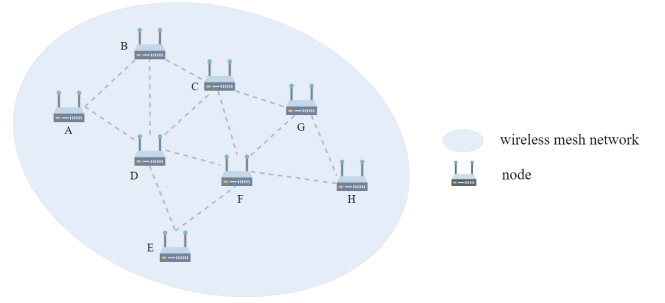


Fig. 3. Mesh network structure. Adapted from [25]

disadvantage of existing wireless networks that are vulnerable to line of sight (LOS) by supporting non-line of sight (NLOS) connectivity [33]. Also it is possible to cover a wide area by interconnecting the multiple mesh networks [29].

*D. Drone detection method*

*1) TinyML, TensorFlow Lite for Microcontrollers:* Tiny Machine Learning (TinyML) allows to implement ML tasks on microcontroller and other low-memory devices [30]. TinyML has several advantages: communication, data privacy and efficient energy. Generated data by the device does not have to leave the device, which helps to reduce communication latency and preserve data privacy. TensorFlow Lite for Microcontrollers (TFLM) is open-source framework for running machine learning models [31]. TFLM makes it easy to deploy TinyML models on a device. The framework is implemented in C++ and supports Arduino library and a specific 32-bit platform. It is also available to be ported to a ESP32 architecture board. This paper utilizes TFLM on the ESP32-WROVER for drone detection. There are two steps for converting TensorFlow (TF) model to run on the device. First, train a TF model and convert it to C-style array. Second, run converted C-style model on the device using C++ TensorFlow Lite library for detection inference.

*2) Object detection:* Convolutional Neural Network (CNN) is suited for object detection because its receptive field effectively capture local features in data [32]. The convolutional layer generates features from receptive field of input data by sharing the convolution kernel. These reduce the number of parameters required for training the model and complexity.

*3) Model optimization:* Edge device typically has limited memory and computational power. In edge device, various optimization methods are applied to reduce model size and resource usage. Quantization, example of model optimization, coverts precision of model weight parameters to a lower precision. By reducing the precision of weight parameters, model size, memory usage and computation cost can be reduced, making it feasible to run the model on an edge device. A model that used 32-bit floating point number reduces model size by converting to 8-bit int or 16-bit int.
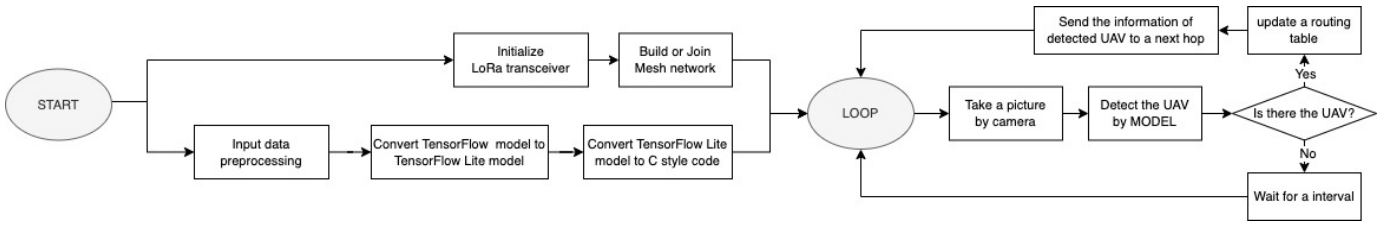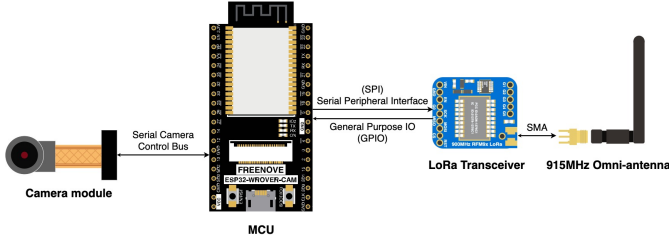
Fig. 4. Block diagram of the system
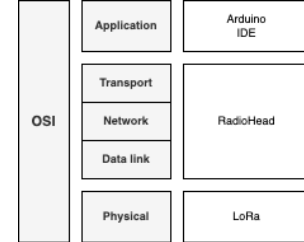


Fig. 5. Hardware structure of the system



Fig. 6. OSI network layers of the system

## IV. IMPLEMENTATION

The system uses observer drones to detect unidentified aerial object as shown in Fig. 1. The observer drones are equipped with a camera, MCU, and LoRa transceiver. The camera records the surrounding of drone always and MCU predict the existence of unidentified object by the recorded image at regular intervals. Each of the drone builds LoRa mesh network, playing a role of network node. The prediction result is transmitted by LoRa transceiver and shared through a mesh network.

### A. System development

*1) Hardware:* ESP32-WROVER MCU board is used to run the system, including communication and detection. This board provides several communication interfaces, such as Serial Peripheral Interface (SPI) and General Purpose IO (GPIO). The structure of hardware is shown in Fig. 5. Camera module, OV2640 is connected by serial control bus port for camera. As the board do not have LoRa module, external LoRa transceiver, RFM95W from Adafruit is connected by wires through male pins of the board. The board transmits the data through SPI and transceiver transmits interrupt signals through GPIO. 915MHz omnidirectional antenna is soldered in transceiver with SMA adapter. Since the board have micro-b port for power supply and uploading code, any type of battery is compatible. Although MCUs derived from ESP chip offer native software platform, ESP-IDF, software of the system is implemented based on Arduino IDE for compatibility with open source libraries.

*2) Network:* LoRa mesh network through multi-hop is implemented for communication within the system. The board is programmed to play a role of hop in mesh network and build a mesh network. Fig. 6 shows proposed network stacks

of the board. RadioHead is packet radio library based on Arduino to send and receive packetized data on embedded Micro-Processor Unit (MPU). Manager class in RadioHead builds a mesh network in the constructor and provides the functions to transmit and receive the data. Driver class has the interfaces to configure LoRa transceiver setting, such as transmission power, frequency, and LoRa parameters. Four recommended options to set the LoRa parameters depend on the purpose is provided. SF and CR are the main factors which affect the performance [36] and high date rate is not essential for the system as text based information of detected UAV is transmitted. The system uses high SF and CR to communicate stably even at a long distance.

Table I lists the specifications of radio which are configured by RadioHead. LoRa modulates the data by 4096 chirps per a symbol, adding 4 bits of error correcting data. Transceiver transmits the signal at a power of 20dBm over 915MHz by omnidirectional antenna which have 5dBi gain.

TABLE I
RADIO SPECIFICATIONS FOR THE DRONE COMMUNICATION

| Specification | value |
|---|---|
| Modulation scheme | LoRa |
| Frequency | 915MHz |
| Transmission power | 20dBm |
| Bandwidth | 125kHz |
| Coding rate | 4 |
| Spreading factor | 4096 chips/symbol |
| Receiver sensitivity | -144dBm |
| Antenna directivity | Omnidirectional antenna |
| Antenna gain | 5dBi |

*3) Detection:* The ESP32-WROVER board has small memory to store data and run code. Usually, in Arudnio, a TF model is stored as a global variable for executing code

until process terminates. These take significant amount of memory. Therefore, small and simple detection model is designed for operating drone detection tasks on the system with simple CNN structure. The network was implemented with TensorFlow Keras library and consist of several layer: two convolution layers, one batch normalization layer, one average pooling layer, flatten layer, two dense layers and two drop layers. The convolution layers extract feature maps of input, while batch normalization layer normalizes output of convolution layer. Global average pooling reduces feature map size to reduce model size. To get four output vales, flatten layer flattens multi-dimensional feature maps to one dimension. To prevent overfitting, dropout layer is used. The output value represent coordinates of bounding box on drone. Fig. [not yet: strucutre of NN] is represent structure of detection model.

In order to deploy TensorFlow model to ESP32-WROVER board, TF model is converted in two steps: converting TF model to TensorFlow Lite (TFL) model and converting TFL model to C-style code. Fist step is conducted with TF library converter. TF model is written to tflite file. Second, TFL model is converted to C-style code by using linux xxd command which convert file to binary data. The binary data is used to Arduino code for performing prediction. Fig. 5 is implementation flow chart of detection.

### B. Performance evaluation

Three experiments were conducted to evaluate the performance of the designed system. The power consumption test confirmed the effect of LoRa on the power efficiency of each drone and the possibility of on-board detection on the low-power MCU. The communication quality test measured the link budget in restrict environment and evaluates the quality of implemented LoRa mesh network by comparing with an estimated link budget. The detection test evaluated the drone detection model based on three criteria, drone detection accuracy, drone inference latency and whether the model is executable on each drones.

*1) Communication quality:* The purpose of this experiment is evaluating a quality of communication within the system.

LoRa have a potential to communicate up to 5km away in urban areas and up to 15km away in rural area since NLOS environment has an impacts on communication distance [37]. On the other hand, the communication of the system have a ability to secure a LOS space, since the observer drones operate at a high enough height. LOS space where a primary radio propagates is called the fresnel zone. Fresnel zone is formed in the shape of a prolate spheroid between a transmitter and a receiver. A radius of fresnel zone is obtained from a equation (1). Where $D$ is the distance between a transmitter and a receiver in km, $f$ is a frequency in GHz.

$$R = 17.31 \times \sqrt{\frac{D}{4 \times f}} \qquad (1)$$
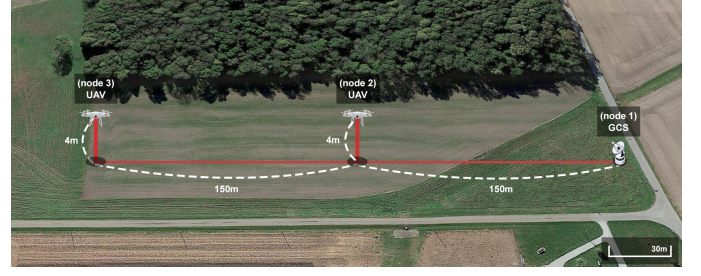


Fig. 7. A wide flatland where three nodes are deployed to measure a link budget of 150m communication. Adapted from [25].
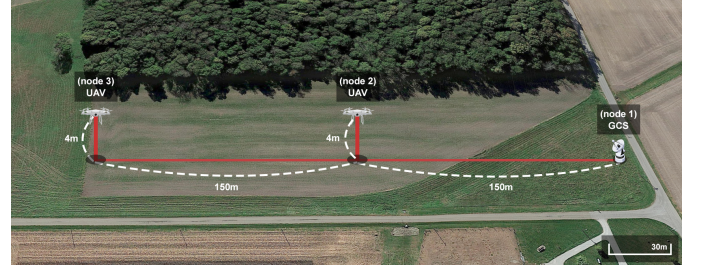


Fig. 8. A wide flatland where three nodes are deployed to measure a link budget of 300m communication. Adapted from [25]. [THIS WILL BE CHANGED]

Two experiments was performed in Fig. 7 and Fig. 8. One base station and two drones was deployed to measure a link budget of UAV-to-Ground (U2G) communication and UAV-to-UAV (U2U) communications. The base stations was installed on the ground and the drones was hovering at an altitude higher than the radius of fresnel zone. Every node requested the packet transmission to every other node to measure a link budget. Air nodes transmitted the routing table to ground node to inspect the multi-hop communication and monitor the status of mesh network. The log of all operations was recorded in a flesh memory of the node which ran the operation.

The results of the two scenarios were measured as shown in Table II. It is necessary to calculate the maximum distance through them to check the network coverage of our system. Link budget shows the performance of a wireless communication channel and figures out if communication works well when it is compared to receiver sensitivity. If the link budget becomes smaller than the receiver sensitivity, it is not allowed to detect the signal, so they are disconnected. The link budget before disconnection has a link with maximum distance, and thereby it is possible to evaluate the network coverage.

$$L = P_t - cableloss + A_t - pathloss + A_R \qquad (2)$$

TABLE II
THE MEASUREMENT OF A LINK BUDGET IN THE EXPERIMENTS FOR
COMMUNICATION QUALITY

| Distance | node1 to node2 | node2 to node1 | node2 to node3 | node3 to node2 |
|---|---|---|---|---|
| 100m | -80.96dBm | -86dBm | -87.09dBm | -82.17dBm |
| 200m | -97.78dBm | -90.18dBm | -90.86dBm | -90.97dBm |

The transmitter power, $P_t$ in dBm is used for the link budget calculation. $A_t$ and $A_r$ mean transmitting antenna gain and receiver antenna gain in dBi respectively. Loss that occurs during communication, such as cable loss and path loss in dB, is also a factor in equation (2). The results of the test are shown in Fig. 7 and Fig. 8, measured differently in the two cases. As the distance between the two nodes increased, the path loss increased, resulting in a difference between the two link budgets. The difference of them indicated the path loss that occurred when the nodes were 100m apart, and it meant the path loss increased by 0.194dB per 10m. The receiver sensitivity was obtained as -144dBm by using the fact that the receiver sensitivity of the LoRa transceiver used in the system is reduced to -144dBm. The minimum link budget not smaller than receive sensitivity was -144dBm and the increment in pathloss was calculated through the difference from the -86.57dBm, link budget in the 200m experimental environment. Therefore the maximum distance of our system was 3.16km when the pathloss increased by 0.194dB per 10m. Additionally, the power consumption of each board was measured in the mesh network. By using a power meter, the power that the board consumed from the battery was calculated when sequentially the ESP32 board, a power meter and a power bank were connected. The standby power while the network was connected was 76mA, and the power when transmitting and receiving the data rose to 109mA.

*2) Detection experiment:* Due to the limited hardware resources of the system, the drone detection model have low detection accuracy and high inference latency. Therefore, this experiment focused on confirming whether the detection model was executed on the system than detection accuracy and inference latency evaluation. The experiment was divided into two parts: experiment setting, result.

The experiment setting is divided into two steps: preprocessing data and training detection model. Drone dataset [39] is used to train detection model. This dataset is newly labeled that was originated from unlabeled 4000 drone images for Amateur Drone Detection and Tracking Project in 2019 [40]. This labeled dataset has 1300 drone images and their annotation XML files. The annotation files have only 1 class to represent wheter object is drone or not. The dataset for experiment was resized to $48 \times 48$ pixels to reduce the input data size and annotation XML files were converted to CSV format. In order to train model, adam optimizer was used to improve learning rate and training stability. Mean Squared Error (MSE) was used to minimize the difference between a predicted value and a real value for updating model weights. After training the detection model, the trained model was applied to the hardware system. The performance experiment was conducted to detect drones while fixing location of the system every $100ms$. This experiment designed with the hypothesis that if the predicted result is correct such for $0.3s$, then it verify that the TensorFlow model is working properly in the system.

The result of the experiment is that the TF model was executed properly on the system when a drone was correctly detected for $0.4s$. Also, the power consumed on the ESP32 board during detecting the drones was measured by using the power meter. On average, the standby power when the detection model was implemented was 85mA, and the peak power increased to 103.5mA.

## V. Conclusion

In this paper, power efficient and long range ACDS is proposed. In field experiment to evaluate a communication performance, the implemented network demonstrated a maximum communication range of 3.16km. The UAV Detection model was successfully operated on low-power MCU from the experiment for detection evaluation. The power consumption of functions was similar to a power consumption of typical MCU. However, simultaneous operation of networking and detection was unsuccessful. The on-chip Static RAM (SRAM) which is used flexibly was only 520kb and Arduino was not possible to utilize a Pseudo Static RAM (PSRAM) for detection although the board has a 8mb PSRAM. The system which is run by a board with a larger SRAM or uses a smaller detection model has a ability to integrate a networking and detection. Furthermore, more datasets and more efficient model guarantee higher accuracy. These potentials of the system for functional integration and improvement are left as future plan.

## References

[1] Y. Zeng, R. Zhang and T. J. Lim, "Wireless communications with unmanned aerial vehicles: opportunities and challenges," in IEEE Communications Magazine, vol. 54, no. 5, pp. 36-42, May 2016.

[2] S. G. Jones, J. Thompson, D. Ngo , J. S. Bermudez Jr, and B. McSorley, "The Iranian and Houthi War against Saudi Arabia," CSIS, Accessed: Feb 10, 2023. [Online]. Available: https://www.csis.org/analysis/iranian-and-houthi-war-against-saudi-arabia

[3] D. Peleschuk, "Russia targets Ukraine in new drone attack," Reuters, Accessed: Feb 10, 2023. [Online]. Available: https://www.reuters.com/world/europe/russia-launched-16-drones-overnight-ukrainian-air-force-2022-12-30/

[4] R. Berg. "Iran blames Israel for Isfahan drone attack, warning of revenge." BBC. https://www.bbc.com/news/world-middle-east-64460139 (accessed Feb. 01, 2023).

[5] B. Galkin, J. Kibilda, and L. A. DaSilva, "UAVs as mobile infrastructure: Addressing battery lifetime," IEEE Commun. Mag., vol. 57, no. 6, pp. 132–137, Jun. 2019.

[6] O. M. Bushnaq, M. A. Kishk, A. Çelik, M.-S. Alouini, and T. Y. Al-Naffouri, "Optimal deployment of tethered drones for maximum cellular coverage in user clusters," 2020, arXiv:2003.00713. [Online]. Available: http://arxiv.org/abs/2003.00713

[7] X. Shi, C. Yang, W. Xie, C. Liang, Z. Shi and J. Chen, "Anti-Drone System with Multiple Surveillance Technologies: Architecture, Implementation, and Challenges," in IEEE Communications Magazine, vol. 56, no. 4, pp. 68-74, April 2018, doi: 10.1109/MCOM.2018.1700430.

[8] "Anti-UAV Defence System," Verdict Media Limited, London, United Kingdom, 2015. [Online]. Available: https://www.homelandsecurity-technology.com/projects/anti-uav-defence-system-auds/

[9] P. Andraši, T. Radišić, M. Muštra, and J. Ivošević, "Night-time Detection of UAVs using Thermal Infrared Camera," Transportation Research Procedia, vol. 28, pp. 183–190, 2017, doi: 10.1016/j.trpro.2017.12.184.

[10] R. Opromolla, G. Fasano, and D. Accardo, "A Vision-Based Approach to UAV Detection and Tracking in Cooperative Applications," Sensors, vol. 18, no. 10, p. 3391, Oct. 2018, doi: 10.3390/s18103391.

[11] A. Chakrabarty, R. A. Morris, X. Bouyssounouse, and R. Hunt, "An Integrated System for Autonomous Search and Track with a small Unmanned Aerial Vehicle," AIAA Information Systems-AIAA Infotech @ Aerospace, Jan. 2017, doi: 10.2514/6.2017-0671.

[12] Espressif Systems. *ESP32 Series Datasheet*, (2023). Accessed: Feb. 10, 2023. [Online]: https://www.espressif.com/sites/default/files/documentation/esp32_datasheet_en.pdf

[13] Espressif Systems. *ESP32-WROVER Series*, (2022). Accessed: Feb. 10, 2023. [Online]: https://www.espressif.com/sites/default/files/documentation/esp32-wrover_datasheet_en.pdf

[14] John A. Volpe National Transportation System Center, "Unmanned Air craft System (USA) Service Demand 2015-2035," 2013. Accessed: Feb. 10, 2023. [Online]. Available: https://irp.fas.org/program/collect/service.pdf

[15] A. Sergeev. "Unsurpassed weapons: Ukrainian kamikaze drones (loitering munition) ST-35 Grom and RAM." gagadget.com. https://gagadget.com/en/0how-it-works/124019-unsurpassed-weapons-ukrainian-kamikaze-drones-loitering-munition-st-35-grom-and-ram/ (accessed Feb. 10, 2023).

[16] D. Hambling. "How Ukraine Perfected The Small Anti-Tank Drone." Forbes. https://www.forbes.com/sites/davidhambling/2022/06/01/how-ukraine-perfected-the-small-anti-tank-drone/?sh=4004e4583171 (accessed Feb. 10, 2023)

[17] "U.S. Standard Atmosphere, 1976," National Oceanic and Atmospheric Administration, USA. Accessed: Feb. 10, 2023. [Online]. Available: https://www.ngdc.noaa.gov/stp/space-weather/online-publications/miscellaneous/us-standard-atmosphere-1976/us-standard-atmosphere_st76-1562 .pdf

[18] Semtech Co. *AN1200.22 LoRa™ Modulation Basics*. (2015), Accessed: Feb. 9, 2023. [Online]. Available: https://semtech.my.salesforce.com/sfc/p/#E0000000JelG/a/2R0000001OJa/2BF2MTeiqIwkmxkcjjDZzalPUGlJ76lLdqiv.30prH8

[19] A. Mondal, M. Hanif and H. H. Nguyen, "SSK-ICS LoRa: A LoRa-Based Modulation Scheme With Constant Envelope and Enhanced Data Rate," in IEEE Communications Letters, vol. 26, no. 5, pp. 1185-1189, May 2022, doi: 10.1109/LCOMM.2022.3150666.

[20] A. Augustin, J. Yi, T. Clausen, and W. Townsley, "A Study of LoRa: Long Range amp; Low Power Networks for the Internet of Things," Sensors, vol. 16, no. 9, p. 1466, Sep. 2016, doi: 10.3390/s16091466.

[21] S. M. Mukhamadiev, E. M. Dmitriyev, E. V. Rogozhnikov, N. V. Duplishcheva and Y. V. Kryukov, "The Effect of Frequency Offset on the Probability of Bit and Packet Errors in Processing Signals with Chirp Spread Spectrum Modulation," 2021 International Siberian Conference on Control and Communications (SIBCON), Kazan, Russia, 2021, pp. 1-5, doi: 10.1109/SIBCON50419.2021.9438858.

[22] Semtech Co. *SX1276/77/78/79 - 137 MHz to 1020 MHz Low Power Long Range Transceiver Datasheet*. (2020), Accessed: Feb. 9, 2023. [Online]. Available: https://semtech.my.salesforce.com/sfc/p/#E0000000JelG/a/2R0000001Rbr/6EfVZUorrpoKFfvaF_Fkpgp5kzjiNyiAbqcpqh9qSjE

[23] Semtech Co. *SX1272/73 - 860 MHz to 1020 MHz Low Power Long Range Transceiver Datasheet*. (2019), Accessed: Feb. 9, 2023. [Online]. Available: https://semtech.my.salesforce.com/sfc/p/#E0000000JelG/a/440000001NCE/v_VBhk1IolDgxwwnOpcS_vTFxPfSEPQbuneK3mWsXlU

[24] F. Costa, S. Genovesi, A. Monorchio and G. Manara, "Low-Cost Metamaterial Absorbers for Sub-GHz Wireless Systems," in IEEE Antennas and Wireless Propagation Letters, vol. 13, pp. 27-30, 2014, doi: 10.1109/LAWP.2013.2294791.

[25] Feb. 11, 2023. [Online]. Available: https://www.freepik.com/

[26] D. Zorbas, G. Z. Papadopoulos, P. Maille, N. Montavont, and C. Douligeris, "Improving LoRa Network Capacity Using Multiple Spreading Factor Configurations," 2018 25th International Conference on Telecommunications (ICT), Jun. 2018, doi: 10.1109/ict.2018.8464901.

[27] R.Riggio, N.Scalabrino, D.Miorandi, G.Iacovoni, "Wireless mesh networks: state of the art and research directions," Create-Net, Apr. 21, 2006. Accessed: Feb. 14, 2023. [Online]. Available: https://citeseerx.ist.psu.edu/document?repid=rep1type=pdfdoi=09ef7b03e0970af477911dac6927515b00088c8f

[28] IBM "What is networking?," ibm.com. Accessed Feb. 14, 2023. [Online]. Available: https://www.ibm.com/topics/networking

[29] M. Gao, F. Zhang and J. Tian, "Environmental Monitoring System with Wireless Mesh Network Based on Embedded System," 2008 Fifth IEEE International Symposium on Embedded Computing, Beijing, China, 2008, pp. 174-179, doi: 10.1109/SEC.2008.28.

[30] R. David et al., "TensorFlow Lite Micro: embedded machine learning on tinyml systems," arXiv preprint arXiv:2010.08678, 2020. [Online]. Available: http://arxiv.org/abs/2010.08678.

[31] TensorFLow. *TensorFlow Lite for Microcontrollers*, Accessed: Feb. 18, 2023. [Online]: https://www.tensorflow.org/lite/microcontrollers

[32] W. Zhiqiang and L. Jun, "A review of object detection based on convolutional neural network," 2017 36th Chinese Control Conference (CCC), Dalian, China, 2017, pp. 11104-11109, doi: 10.23919/ChiCC.2017.8029130.

[33] Karthika K.C, "Wireless mesh network: A survey," 2016 International Conference on Wireless Communications, Signal Processing and Networking (WiSPNET), Chennai, India, 2016, pp. 1966-1970, doi: 10.1109/WiSPNET.2016.7566486.

[34] G. Chand, M. Lee, and S. Shin, "Drone Based Wireless Mesh Network for Disaster/Military Environment," Journal of Computer and Communications, vol. 06, no. 04, pp. 44-52, Apr. 26, 2018. Accessed: Feb. 17, 2023. doi: 10.4236/jcc.2018.64004. [Online]. Available: https://www.scirp.org/pdf/JCC_2018042515455922.pdf

[35] L. Davoli, E. Pagliari, G. Ferrari, "Hybrid LoRa-IEEE 802.11s Opportunistic Mesh Networking for Flexible UAV Swarming," Drones, vol. 5, no. 2, pp. 1-33, Apr. 15. Accessed: Feb. 17, 2023. [Online]. Available: https://www.mdpi.com/2504-446X/5/2/26

[36] A. S. Kurji, A. H. Al-Nakkash, and O. A. Hussein, "LORA in a Campus: Reliability and Stability Testing," IOP Conference Series: Materials Science and Engineering, vol. 1105, no. 1, p. 012034, Jun. 2021, doi: 10.1088/1757-899x/1105/1/012034.

[37] Semtech Co. *What are LoRa® and LoRaWAN®?*, Accessed: Feb. 18, 2023. [Online]. Available: https://lora-developers.semtech.com/documentation/tech-papers-and-guides/lora-and-lorawan/

[38] Feb. 18, 2023. [Online]. Available: https://www.flaticon.com/

[39] Drone Dataset (UAV), 2020. [Online]. Available: https://www.kaggle.com/datasets/mcagriaksoy/amateur-unmanned-air-vehicle-detection-dataset

[40] Drone Dataset: Amateur Unmanned Air Vehicle Detection, Nov. 25 2019, doi: 10.17632/zcsj2g2m4c.4